

High-Temperature Chemistry and Oxidation of ZrB₂ Ceramics Containing SiC, Si₃N₄, Ta₅Si₃, and TaSi₂

Inna G. Talmy,[†] James A. Zaykoski, and Mark M. Opeka

Naval Surface Warfare Center Carderock Division (NSWCCD), West Bethesda, Maryland 20817-5700

The effect of Si₃N₄, Ta₅Si₃, and TaSi₂ additions on the oxidation behavior of ZrB₂ was characterized at 1200°–1500°C and compared with both ZrB₂ and ZrB₂/SiC. Significantly improved oxidation resistance of all Si-containing compositions relative to ZrB₂ was a result of the formation of a protective layer of borosilicate glass during exposure to the oxidizing environment. Oxidation resistance of the Si₃N₄-modified ceramics increased with increasing Si₃N₄ content and was further improved by the addition of Cr and Ta diborides. Chromium and tantalum oxides induced phase separation in the borosilicate glass, which lead to an increase in liquidus temperature and viscosity and to a decrease in oxygen diffusivity and of boria evaporation from the glass. All tantalum silicide-containing compositions demonstrated phase separation in the borosilicate glass and higher oxidation resistance than pure ZrB₂, with the effect increasing with temperature. The most oxidation-resistant ceramics contained 15 vol% Ta₅Si₃, 30 vol% TaSi₂, 35 vol% Si₃N₄, or 20 vol% Si₃N₄ with 10 mol% CrB₂. These materials exceeded the oxidation resistance of the ZrB₂/SiC ceramics below 1300°–1400°C. However, the ZrB₂/SiC ceramics showed slightly superior oxidation resistance at 1500°C.

I. Introduction

THE unique combination of properties (high melting temperature, high hardness and strength, good oxidation resistance, and high thermal conductivity) makes ceramics based on ZrB₂ and HfB₂ promising candidates for high-temperature applications^{1–7} such as hypersonic vehicle aerosurfaces (leading edges and nosecones), which require oxidation resistance at temperatures above 2000°C.

The good oxidation resistance of pure Zr and Hf diborides is a result of the formation of an oxidation product consisting of ZrO₂ (HfO₂) and B₂O₃. Below 1200°C liquid boria fills all of the porosity in the fine-grained oxides, providing oxidation protection. However, above 1200°C the diborides oxidize rapidly as a result of the evaporation of the protective B₂O₃ from the oxide scale. It should be noted that a fraction of boria (about 15 vol%) remains within the oxide scale at temperatures up to 1500°C because of the high surface tension of the porous, fine-grained ZrO₂ layer.⁸ The presence of liquid boria explains the superior oxidation resistance of these borides compared with the corresponding carbides and nitrides, which form single-phase, porous ZrO₂ scales as a result of the formation of gaseous oxidation products.

In general, the oxidation behavior of non-oxide ceramics largely depends on the chemical composition and properties of the oxidation products and on the combination of physical and chemical processes taking place on the surface exposed to oxygen-containing atmosphere. Modification of the chemical com-

position of the oxide layer, leading to decreased inward diffusion of oxygen, is an effective way of controlling oxidation resistance of nonoxide ceramics. This modification can be accomplished by changing the bulk composition of ceramics.

Numerous studies dedicated to the improvement of the oxidation resistance of ZrB₂ and HfB₂^{2,5,6,9–15} resulted in the selection of ceramics with 20–30 vol% SiC as optimal, preferred compositions. The SiC-containing ZrB₂ ceramics showed relatively high oxidation resistance up to 1500°C as a result of the formation of the protective surface layer of borosilicate glass. Compared with liquid B₂O₃, the borosilicate glass has higher melting temperature, higher viscosity, and lower oxygen diffusivity, thus providing much more effective oxidation protection. Theoretical aspects of the oxidation behavior of the zirconium boride-based materials have been reported earlier.¹

The increase in the oxidation resistance of ZrB₂/25 vol% SiC ceramics was accomplished by the addition of CrB₂, TiB₂, TaB₂, NbB₂, and VB₂ (as substitution for ZrB₂),¹⁶ despite the fact that the oxidation resistance of all the modifying diborides (alone) is much worse than that of the ZrB₂ and HfB₂.^{17,18} This improvement in the oxidation resistance was related to the presence of transition metal oxides (as a result of the oxidation of the corresponding diborides) in the borosilicate glass inducing its phase separation (immiscibility). Both increased liquidus temperatures and viscosities, which are characteristic features of immiscible glasses, and are beneficial for decreasing oxygen diffusivity and suppressing boria evaporation from the glass.

The effectiveness of oxides in enhancing immiscibility increases with increasing metallic element cation field strength, z/r ,² where z is the valence and r is the ionic radius.^{19–22} Because the cation field strengths of Ti, Nb, Ta, Mo, Cr, and V are higher than that of Zr, these elements are effective in promoting phase separation of the ZrO₂-containing borosilicate glass.

Studies on the effect of alternative sources of Si (instead of SiC), such as Si₃N₄ and silicides, on the oxidation behavior of ZrB₂ ceramics are not systematic and are sometimes contradictory. Bellosi and Monteverde²³ reported an increase in the oxidation resistance of ZrB₂ ceramics at 1350° and 1600°C with the addition of 5 vol% Si₃N₄. During hot pressing at 1700°C, Si₃N₄ decomposed with the formation of BN, ZrO₂ and a B–N–O–Zr–Si glassy phase. Unlike the previous data, Sato *et al.*²⁴ did not observe any chemical interaction between Si₃N₄ fibers and the ZrB₂ matrix after hot pressing at 1400°C.

The effect of the disilicides of Ta, Nb, W, Mo, and Zr, as well as of Zr₅Si₃ on the oxidation resistance of ZrB₂ was studied by Shaffer.^{25,26} In these studies, ZrB₂ ceramics containing 5–15 mol% MoSi₂ showed superior oxidation performance at both 1400° and 1950°C. Shaffer also suggested the addition of ZrB₂/5–50 mol% TaSi₂ mixture as oxidation-protective coatings for Mo, borides, and carbides. An increase in the oxidation resistance of ZrB₂ up to 1200°C with the addition of ZrSi₂ was reported by Lavrenko *et al.*²⁷ The authors also found solid solubility between the components after pressureless sintering in vacuum (no sintering temperature was given). Panasyuk *et al.*²⁸ reported an improvement in oxidation resistance of ZrB₂ with the addition of 15–50 wt% CrSi₂. The experiments were conducted at 600°–1200°C and 740 torr (98.6 kPa) oxygen

N. Jacobson—contributing editor

Manuscript No. 24005. Received November 19, 2007; approved February 8, 2008.

[†]Author to whom correspondence should be addressed. E-mail: inna.talmy@navy.mil

pressure for 120 min. The improvement in oxidation resistance was attributed to the formation of protective ZrSiO₄.

Pastor and Meyer²⁹ evaluated the oxidation resistance of ZrB₂ with additions of MSi₂ or M₅Si₃, where M is a transition metal Zr, Ta, Cr, Mo, or W. The authors observed significant interactions or solid solubility in the systems of ZrB₂ with Zr, Cr, and Mo silicides and very little or no interactions in the systems with Ta and W silicides. After oxidation testing for up to 100 h at 1200° and 1400°C, the ZrB₂/15 wt% CrSi₂ composition was the most oxidation resistant. Opila *et al.*³⁰ reported that the addition of 20 vol% TaSi₂ to ZrB₂/20 vol% SiC improved the oxidation resistance of the material at 1627°C in air. The improved behavior was attributed to the presence of Ta, not to the increase in Si content as a result of the introduction of the second Si-containing component. The processing, chemical interactions, and properties of ceramics in the whole ZrB₂/Ta₅Si₃ system were reported by Talmy *et al.*³¹

The purpose of the present work is to characterize the oxidation behavior of ZrB₂ modified with Si₃N₄, Ta₅Si₃, and TaSi₂ as sources of Si and to compare the results with the oxidation behavior of SiC-containing ZrB₂. The introduction of Ta silicides was of particular interest because it simultaneously modifies the oxidation layer with SiO₂ to form borosilicate glass and with Ta₂O₅ to induce glass immiscibility for potential further improvement in oxidation resistance.

The experimental compositions ZrB₂/5, 20, and 35 vol% Si₃N₄, ZrB₂/8, 15, and 31 vol% Ta₅Si₃, and ZrB₂/10, 20, and 30 vol% TaSi₂ were selected to keep the B₂O₃/SiO₂ ratio in the surface borosilicate glass between 1.5 and 3, assuming that ZrB₂ and Si-containing additives are totally oxidized. (This ratio in the ZrB₂/25 vol% SiC composition is 2.) According to the SiO₂-B₂O₃ phase diagram,³² the melting temperature of borosilicate glass of these compositions would be about 600°–700°C. It should be noted that SiO₂ content in glass and glass melting temperatures will gradually increase as B₂O₃ evaporates with increasing oxidation temperature and/or time.

II. Experimental Procedure

The starting borides and silicides (–325 mesh and 99.5% purity) were purchased from Cerac Inc. (Milwaukee, WI). Silicon nitride (LC12, particle size 0.6 μm) was purchased from HC Starck, Inc. (Newton, MA). The powders were mixed with a mortar and pestle in acetone. The mixing procedure was repeated three times with intermediate drying. The materials were densified by hot pressing (Model 912G, Thermal Technology Inc., Santa Rosa, CA) in a graphite mold in He atmosphere. The hot-pressing conditions will be given in the sections corresponding to the specific systems.

The samples were heated to the maximum temperature with a ramp rate of 40°C/min under a pressure of 5 MPa, and the full pressure was applied when the desired densification temperature was reached. The hot-pressed samples were characterized by density and open porosity (Archimedes principle), phase composition (X-ray diffraction (XRD), Siemens Theta/Theta, Model D 500, Bruker AXS, Madison, WI), and microstructure (SEM, Model ISI ABT SR-50A, Withington, Manchester, UK). Energy-dispersive spectroscopy (EDS) was also used to identify the elemental composition of phases. The boron content data were inconclusive and are not reported in the paper.

The oxidation behavior was characterized by measuring mass changes of the bars (average size about 3 mm × 4 mm × 5 mm and surface area about 1.0 cm²) during furnace heating in air at 1000°–1500°C for 2 h. The bars were supported by their ends on alumina semirings for maximum contact with the atmosphere. The mass with and without the semi-rings was recorded to allow posttest mass measurements in the event that the glassy oxidation product reacted with the alumina. The mass change results were an average from three to five samples. Air quenching of the samples after furnace heating was conducted to retain the high-temperature condition of the surface layer for room temperature

X-ray and microscopic evaluations. XRD and SEM/EDS were used to characterize the phase composition and microstructure of the surface and cross-section of the samples after oxidation.

III. Results and Discussion

(1) ZrB₂-Si₃N₄ Ceramics

The ZrB₂ ceramics containing 5–35 vol% Si₃N₄ were prepared by hot pressing mixtures of the end-member powders at 1850 °C and 20 MPa in He for 1 h. Unlike SiC, which is chemically compatible with ZrB₂,³³ Si₃N₄ was decomposed during hot pressing. The XRD analysis showed the presence of BN, ZrSi₂, and ZrN in addition to the residual ZrB₂. The coexistence of ZrSi₂ and ZrB₂ observed in the present research confirms the Brukl phase equilibria data,³⁴ but contradicts the solid solubility data reported by Lavrenko *et al.*²⁷ and Kieffer and Benesovsky.³⁵

The relative densities of the ceramics were not determined because of the unknown quantitative phase composition of the final materials. However, the samples did not have any open porosity. The microstructure of materials containing up to 20 vol% Si₃N₄ in the starting mixtures consists of coarse crystals surrounded by a fine-grained phase (Fig. 1). The EDS analysis showed only Zr in the coarse crystals (presumably ZrB₂) and Zr, Si, and N in the fine-grained phase (ZrB₂, BN, ZrSi₂, and ZrN reaction products). The sizes of both ZrB₂ and fine-phase crystals decrease with increasing Si₃N₄ content, and ceramics containing 35 vol% Si₃N₄ had a uniform fine-grained structure.

The oxidation resistance of the Si₃N₄-containing ceramics during furnace heating increased (but mass gain decreased) with increasing Si₃N₄ (Fig. 2). The lower mass gain for pure ZrB₂ compared with the sample containing 5 vol% Si₃N₄ is due to the significant evaporation of B₂O₃ from pure ZrB₂ above 1200°C, decreasing the total weight gain from the formation of ZrO₂ and B₂O₃ during oxidation. The significantly larger mass gain measured for the 5 vol% Si₃N₄-containing sample in comparison with that for pure ZrB₂ resulted from the lower evaporation of B₂O₃ from borosilicate glass formed on the surface of this sample.

The smaller thickness of the oxidation layer for the 5 vol% Si₃N₄-containing sample (140 μm) compared with that for pure ZrB₂ (160 μm) after 2 h oxidation at 1300°C affirms improved oxidation resistance of ZrB₂ with the addition of even small amounts of Si₃N₄. The data on the formation of the surface glass and improvement in the oxidation resistance of ZrB₂ by the addition of 5 vol% Si₃N₄ support the results reported by Bellosi and Monteverde.²³ The thickness of the oxidized layer for the ZrB₂/20 vol% Si₃N₄ ceramics tested at 1300°C was 60 μm. Only ZrO₂ was identified on the surface of all oxidized Si₃N₄-containing samples.

By analogy with ZrB₂/SiC materials, CrB₂ and TaB₂ were added to the ZrB₂/Si₃N₄ ceramics to induce phase separation in

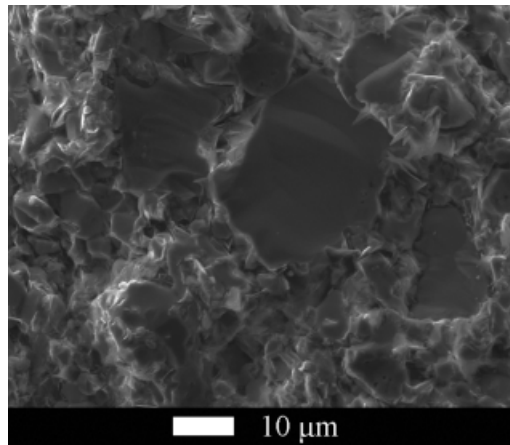


Fig. 1. SEM of ZrB₂/20 vol% Si₃N₄ ceramics hot-pressed at 1850°C and 20 MPa for 1 h.

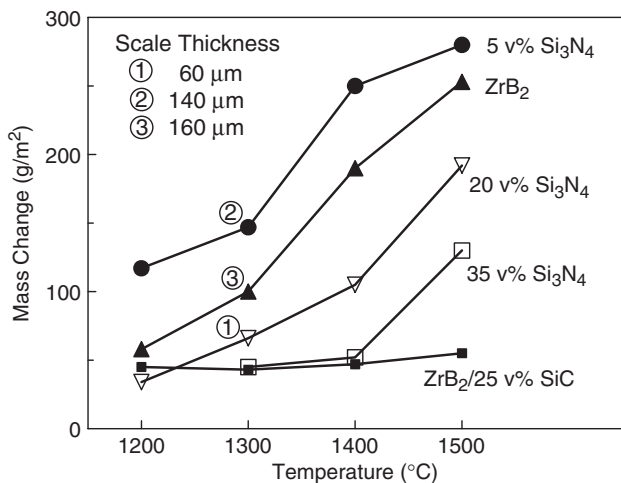


Fig. 2. Mass changes during furnace oxidation (2 h) of $\text{ZrB}_2/\text{Si}_3\text{N}_4$ ceramics at 1200–1500°C.

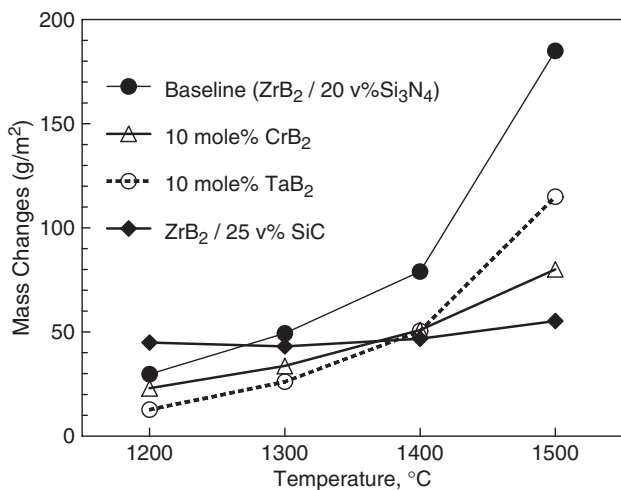


Fig. 3. Mass changes during furnace oxidation (2 h) of $\text{ZrB}_2/20 \text{ vol} \% \text{ Si}_3\text{N}_4$ ceramics modified with 10 mol% CrB_2 and TaB_2 at 1200–1500°C.

the surface glass during the oxidation test. The additives were introduced as a 10 mol% substitution for ZrB_2 with constant 20 vol% Si_3N_4 . No significant changes in the microstructure were observed for the modified ceramics compared with the baseline material. As previously discussed, Si_3N_4 reacted with ZrB_2 during hot pressing with the formation of BN , ZrSi_2 , and ZrN , which were localized in the fine-grained areas. By EDS analysis, the modifying elements were detected only in the fine-grained phase. The dissolution of CrB_2 and TaB_2 in ZrB_2 was determined by XRD. The ZrB_2 peaks were shifted to higher angles, indicating the contraction of the ZrB_2 lattice as a result of the incorporation of CrB_2 and TaB_2 , which have smaller lattice constants than ZrB_2 .

The oxidation behavior of the modified compositions together with that of ZrB_2 with 20 vol% Si_3N_4 and ZrB_2 with 25 vol% SiC ceramics is shown in Fig. 3. The modifying diborides increased the oxidation resistance of the baseline ceramics. The mass gain of the ceramics containing TaB_2 and CrB_2 was 26 and 34 g/m^2 , respectively, compared with 49 g/m^2 for the baseline composition after 2 h oxidation at 1300°C. Higher oxidation resistance of these ceramics at temperatures below 1400°C compared with that of ZrB_2/SiC ceramics can be attributed to the oxidation rate difference between ZrSi_2 (the Si source in these ceramics) and SiC . It is known that SiC does not oxidize appreciably at these lower temperatures to participate in the formation of borosilicate glass.¹⁶ However, ZrSi_2 oxidizes more readily and enhances the low-temperature formation of the protective borosilicate glass. Lavrenko's observation²⁷ of the formation of a vitreous borosilicate film after oxidation of the $\text{ZrB}_2/50 \text{ wt} \% \text{ ZrSi}_2$ material at 700–850°C is consistent with the present results.

The presence of Ta and Cr oxides, which induce phase separation in the glass, further improves glass-protective capabilities. The effect of the additives was very similar at temperatures below 1400°C. Above 1400°C the best oxidation resistance was shown by the CrB_2 -containing material.

Extensive phase separation (mostly “cabbage”-like configurations) was observed on the surface of all the modified samples after oxidation tests. Figure 4 shows the SEM micrograph of the surface of the CrB_2 -containing sample after oxidation at 1300°C for 2 h. The overall XRD of the surface of this sample identified ZrO_2 , Cr_2O_3 , and CrO_2 . The presence of Cr in the Cr^{4+} oxidation state having a high cation field strength (1322 compared with 793 nm^{-2} for Cr^{3+}) contributed significantly to the phase

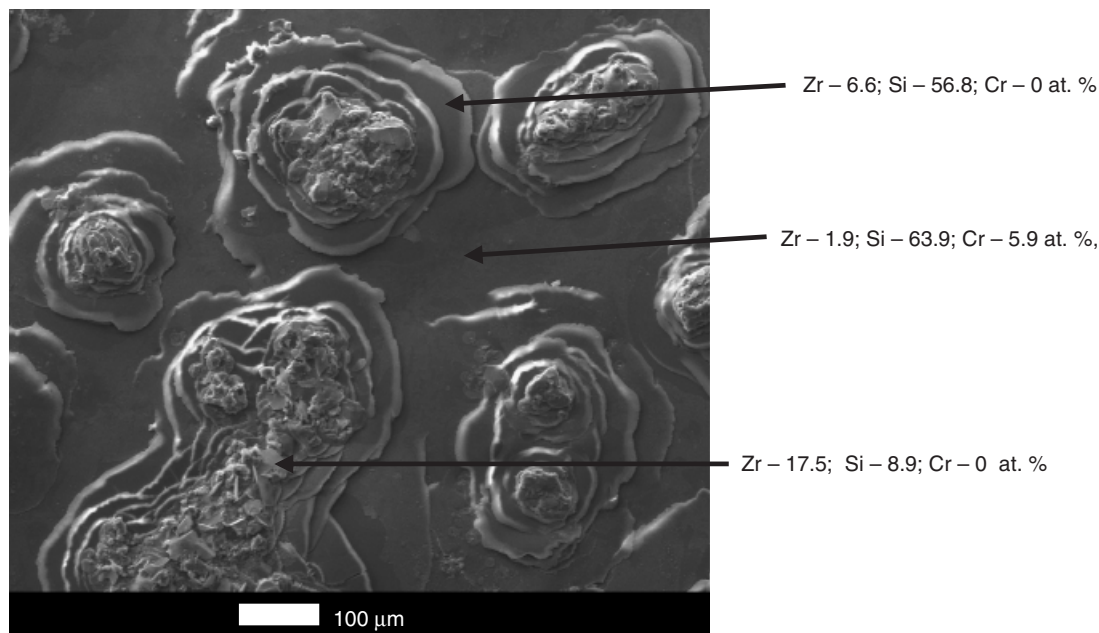


Fig. 4. SEM of the surface of $\text{ZrB}_2/20 \text{ vol} \% \text{ Si}_3\text{N}_4/10 \text{ mol} \% \text{ CrB}_2$ ceramics after oxidation at 1300°C for 2 h.

Table I. Phase Composition of ZrB₂/Ta₅Si₃ Ceramics After Hot Pressing at 1900°C for 30 min

Ta ₅ Si ₃ (tetragonal) content in ZrB ₂ /Ta ₅ Si ₃ starting mixtures		Phases determined by XRD			
Mol%	Vol%	ZrB ₂	ZrB ₂ (ss)	TaB	Ta ₅ Si ₃ (D8 ₈ hexagonal) (ss)
0	0	x			
2	8	x	x		
4	15	x	x		
10	31	x	x	x	x

XRD, X-ray diffraction.

separation in the glass and, subsequently, to the improvement in its oxidation protection capability, which is especially pronounced at temperatures below 1400°C. The EDS analysis of this sample showed a significant concentration of Zr in the top area of the “cabbage” (17.5 at.% compared with 1.9 at.% in the glassy area) and the presence of Cr only in the glass.

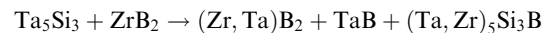
(2) ZrB₂-Ta₅Si₃ Ceramics

ZrB₂ ceramics modified with 8, 15, and 31 vol% (2, 4, and 10 mol%) Ta₅Si₃ were prepared by hot pressing starting mixtures at 1900°C and 20 MPa for 30 min in a graphite mold and He atmosphere. The XRD analysis revealed significant interaction between ZrB₂ and Ta₅Si₃ during hot pressing. The polymorphism of Ta₅Si₃, as well as the chemical interactions and solid solubility in the entire ZrB₂-Ta₅Si₃ system, is described elsewhere.³¹ The phase compositions of the ceramics containing 2, 4, and 10 mol% are summarized in Table I.

The ceramics containing 2 and 4 mol% Ta₅Si₃ consisted of stoichiometric ZrB₂ and ZrB₂-based solid solution with a contraction of the ZrB₂ unit cell. The unit cell volume of ZrB₂ decreased linearly from 30.70 to 29.89 Å³ as Ta₅Si₃ content increased from 0 to 4 mol%. Based on the insolubility of Si and ZrSi_x in ZrB₂ reported in the literature^{34,36} and the contraction observed in the ZrB₂ lattice, it was deduced that Ta entered the ZrB₂ cell, causing the contraction (the atomic radii of Zr and Ta are 1.60 and 1.46 Å, respectively).

The samples containing 10 mol% Ta₅Si₃ also showed the presence of ZrB₂ and ZrB₂-based solid solution. However, the solid-solution unit cell volume only slightly changed with an increase in Ta₅Si₃ content from 4 to 10 mol%. This indicated that the solubility limit of Ta in the ZrB₂ lattice, with the present reactant ratios, was achieved in the material containing about 4 mol% Ta₅Si₃. The simultaneous presence of ZrB₂ and ZrB₂-based solid solutions is probably the result of insufficient time (30 min) during hot pressing to completely homogenize the composition.

Additionally, the samples with 10 mol% Ta₅Si₃ contained substantial amounts of two new phases: TaB and a Ta₅Si₃-based hexagonal (D8₈) solid solution with considerable expansion of the silicite cell volume from 252.77 Å³ (for pure hexagonal Ta₅Si₃) to 273.83 Å³ for the solid solution formed in the material, as determined by XRD. The possible reaction between the components could be presented as a hypothetical equation:

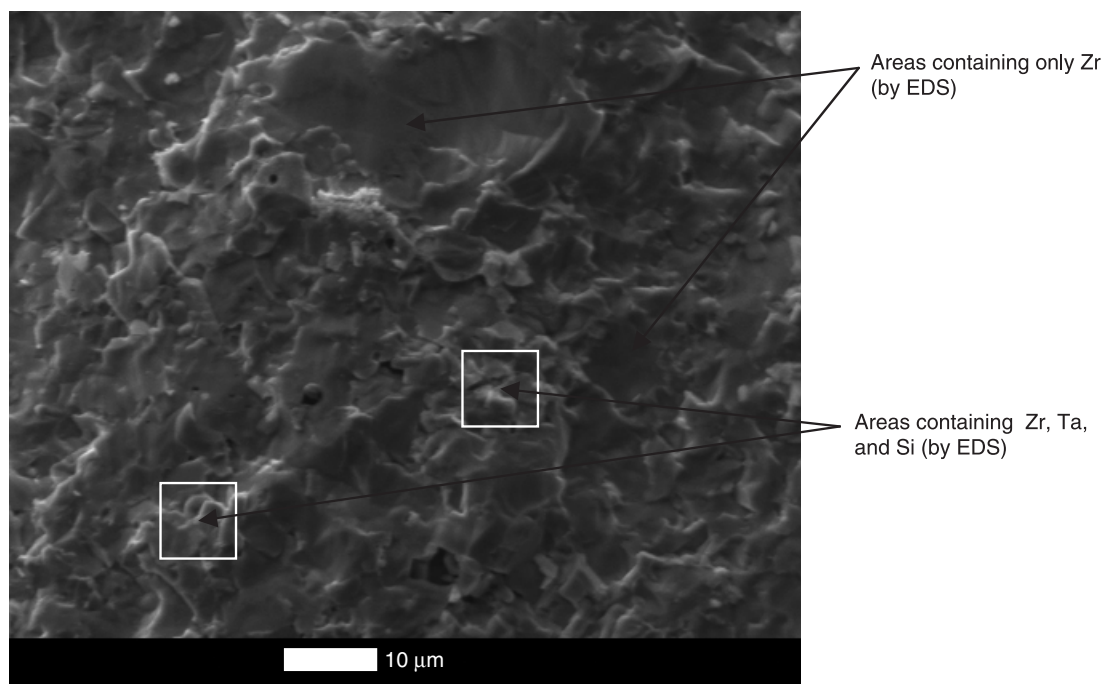


This reaction involved the decomposition of some fraction of the ZrB₂, which provided B for the formation of TaB, as well as Zr and B for the formation of the D8₈-based solid solution. Both the interstitial incorporation of B and the substitution of Ta with Zr resulted in significant D8₈ lattice expansion. It is also noteworthy that the TaB lattice parameters corresponded to the stoichiometric composition, indicating no dissolution of Zr in TaB.

The observed chemical interaction and solid solubility between Ta₅Si₃ and ZrB₂ contradict the only existing literature data,²⁹ which reports that very little or no interaction is observed even after heating at 2200°C and 10⁻² torr (1.33 Pa) for 1 h. This dramatic discrepancy in these two studies is not easy to resolve.

The bulk densities of the samples were 6.61, 7.18, and 8.27 g/cm³ for ceramics containing 8, 15, and 31 vol% Ta₅Si₃, respectively, with close-to-zero open porosity. (The relative densities of the ceramics were not determined because of the unknown quantitative phase composition of the final ceramics.) Evidently, a decrease in the hot pressing temperature of the Ta₅Si₃-containing materials compared with pure ZrB₂ (2200°C) can be related to chemical interactions and solid solubility between the components.

The microstructure of the hot-pressed ZrB₂/15 vol% Ta₅Si₃ sample (Fig. 5) is composed of large crystals (average size about 5–10 μm) containing predominantly Zr (by EDS) surrounded by

**Fig. 5.** SEM of ZrB₂/15 vol%/Ta₅Si₃ ceramics HP at 1900°C.

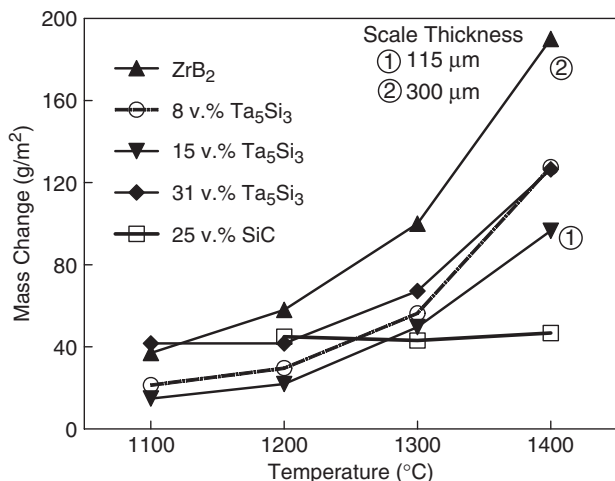


Fig. 6. Mass changes during furnace oxidation (2 h) of ZrB_2 ceramics containing 0, 8, 15, and 31 vol% Ta_5Si_3 at 1100° – $1400^{\circ}C$.

fine-grained crystals (about $1\ \mu m$) consisting of both Zr and Ta, which is an indication that fine ZrB_2 particles preferentially participated in the chemical interactions between the components. The location of Si was difficult to identify because of the overlapping of Ta and Si peaks, but it can be assumed that it was localized in the fine-grained phase.

Figure 6 shows the mass gain for ZrB_2 – Ta_5Si_3 ceramics during 2 h oxidation at 1100° – $1400^{\circ}C$. Materials containing Ta_5Si_3 exhibited increased oxidation resistance, which is further supported by measurements of the thickness of the oxidized layer after oxidation at $1400^{\circ}C$. The thickness of the oxidized layer was $115\ \mu m$ for ceramics containing 15 vol% Ta_5Si_3 compared with $300\ \mu m$ for pure ZrB_2 . The presence of ZrO_2 and $TaZr_{2.75}O_8$ was determined by XRD on the surface of the oxidized samples. No crystalline silicon- or boron-containing compounds were identified with certainty.

A periodic pattern of glassy and crystalline areas on the oxidized surface of the ceramics containing 8 vol% Ta_5Si_3 (Fig. 7) implies glass phase separation, which was induced by the presence of Ta^{5+} . In spite of the overlapping of major Ta and Si peaks, EDS analysis of the surface leads to the conclusion that the glassy area contains a very small amount of Zr and

practically no Ta (from the size of the “far”, $\approx 8\ keV$, Ta peak), while the crystallized area contains Ta and a significant amount of Zr. The strong peak belonging to both Si and Ta in the EDS scan of the glassy area can be therefore associated predominantly with Si, and the peak from the crystallized area of the scan is from a combination of both elements.

Thus, the improved oxidation resistance of the Ta_5Si_3 -containing compositions compared with pure ZrB_2 is due to the formation of an immiscible borosilicate glass during oxidation. The test results of this study did not match the results of Pastor and Meyer,²⁹ who did not observe any improvement in the oxidation resistance of ZrB_2 by the addition of 15 wt% Ta_5Si_3 (the composition corresponds to 8 vol% Ta_5Si_3 in the present study) after oxidation in air at $1200^{\circ}C$ for 100 h.

In spite of the improvement in oxidation resistance of ZrB_2 with the addition of up to 31 vol% Ta_5Si_3 , ZrB_2 ceramics containing 25 vol% SiC have superior oxidation resistance at temperatures above $1300^{\circ}C$, as shown in Fig. 6. The enhanced oxidation resistance of Ta_5Si_3 -containing ceramics below $1300^{\circ}C$ can be attributed to the insufficient oxidation of SiC at these temperatures to form a continuous, protective borosilicate glass, while significant oxidation of Ta_5Si_3 occurred below $1100^{\circ}C$.³¹

(3) ZrB_2 – $TaSi_2$ Ceramics

ZrB_2 ceramics containing 10, 20, and 30 vol% (approximately 7, 15, and 23 mol%, respectively) $TaSi_2$ were prepared by hot pressing at $2000^{\circ}C$ and 20 MPa for 20 min in a He atmosphere. The bulk densities of the samples were 5.63, 6.44, and $6.73\ g/cm^3$, respectively. The XRD patterns of the ceramics showed solid solubility in the system (Fig. 8). The ceramics containing 10 vol% $TaSi_2$ did not show the diffraction peaks of $TaSi_2$. As the amount of $TaSi_2$ increased to 20 and 30 vol%, the $TaSi_2$ peaks became evident and increased in intensity with increasing $TaSi_2$ concentration. The peaks were shifted to the left from the position of the stoichiometric $TaSi_2$, indicating lattice expansion. The diffraction peaks of ZrB_2 were shifted to the right of the expected positions, indicating lattice contraction. The presence of the shoulder corresponding to the position of the stoichiometric ZrB_2 at $2\theta = 41.6^{\circ}$, on the left of the shifted ZrB_2 peak on the pattern of the material containing 20 and 30 vol% $TaSi_2$, probably indicates insufficient processing time to homogenize the phase composition. The calculated unit cell volume decreased for ZrB_2 from 30.70 to $30.02\ \text{\AA}^3$ and increased for

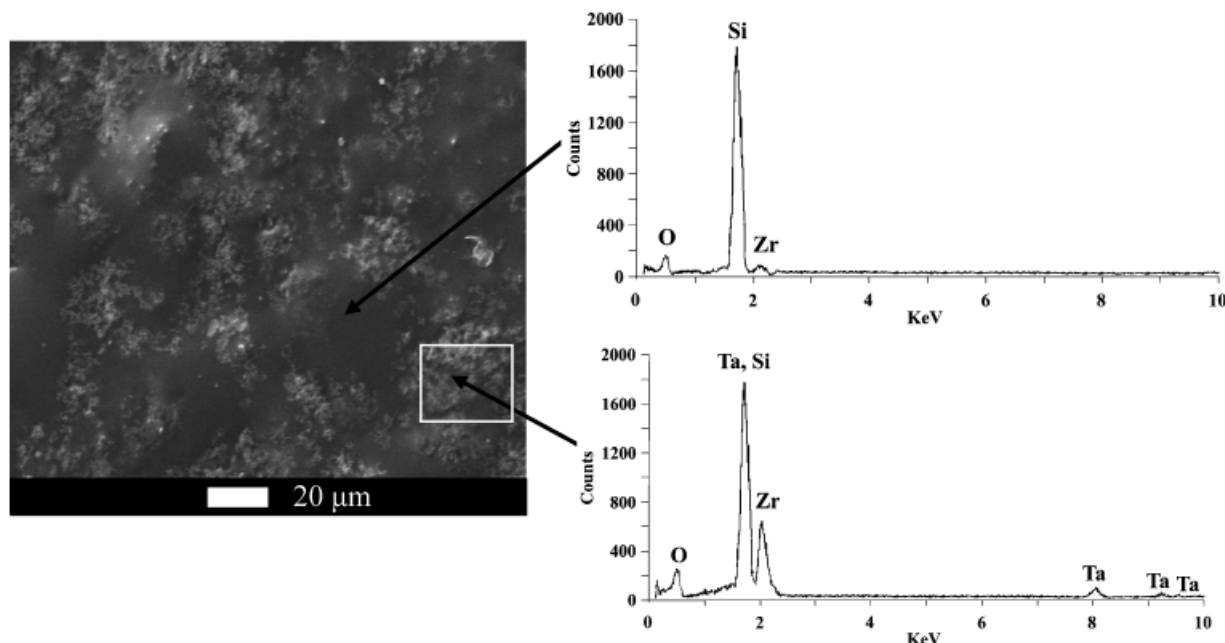


Fig. 7. SEM/EDS of the surface of $ZrB_2/8\ vol\% Ta_5Si_3$ ceramics after oxidation at $1300^{\circ}C$ for 2 h.

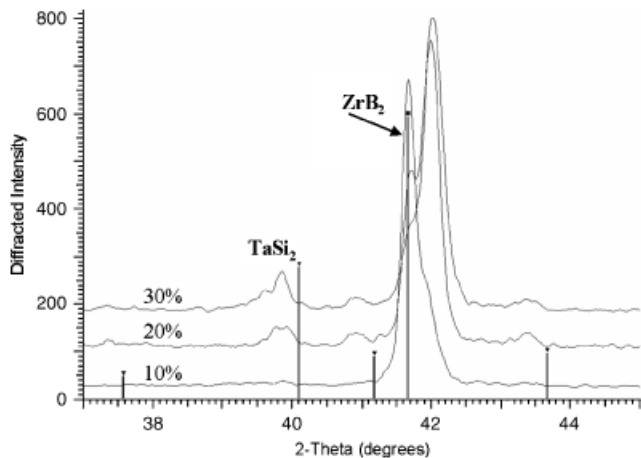


Fig. 8. X-ray diffraction of ZrB₂/10, 20, and 30 vol% TaSi₂ ceramics HP at 2000°C for 20 min.

TaSi₂ from 130.19 to 132.67 Å³ in the ceramics containing 20 vol% (15 mol%) TaSi₂, confirming the formation of solid solutions.

The solid solubility in the system was not expected and was not previously reported in the literature. The crystal structures of both ZrB₂ and TaSi₂ are hexagonal but belong to different space groups (ZrB₂ is AlB₂-type (*P6/mmm*) and TaSi₂ is CrSi₂-type (*P6₂22*)). Based on the results of Brukl's research,³⁴ which excluded solubility of silicon or silicides in ZrB₂, one way to interpret the formation of solid solutions between ZrB₂ and TaSi₂ is to consider that only the transition metals mutually dissolve, leaving the boride and silicide lattices intact. With atomic radii of Zr and Ta being 0.160 and 0.146 nm, respectively, the incorporation of Ta into the ZrB₂ crystal lattice and Zr into the TaSi₂ crystal lattice had to result in the observed contraction of the ZrB₂ and expansion of the TaSi₂ crystal lattices.

A mutual solubility of ZrB₂ and TaSi₂ is supported by the results of SEM/EDS studies, which showed that the majority of the crystals had a core-shell structure with the core being ZrB₂ and the shell containing both Ta and Zr (illustrated on Fig. 9) for ceramics with 30 vol% TaSi₂. It can be assumed that the simultaneous presence (Fig. 8) of the shifted ZrB₂ peaks and the stoichiometric ZrB₂ peak reflects the core/shell structure of the material. It is expected that an increase in holding time during hot pressing would complete the formation of the solid solutions and eliminate the core-shell structure of the crystals.

The oxidation resistance of ZrB₂-TaSi₂ ceramics increased with increasing TaSi₂ content (Fig. 10). Samples containing 10 vol% TaSi₂ showed higher mass gain than pure ZrB₂ at all temperatures. This behavior was also observed for the ZrB₂/5 vol% Si₃N₄ ceramics and was due to the significant evaporation of B₂O₃ from pure ZrB₂ above 1200°C, decreasing the total weight gain from the formation of ZrO₂ and B₂O₃ during oxidation. The ceramics containing 20 and 30 vol% TaSi₂ exhibit significantly less mass gain than ZrB₂ up to 1400°C. The matching values of the mass gain for ZrB₂ and ceramics with 30 vol% TaSi₂ at 1500°C are again the result of extensive evaporation of B₂O₃ from ZrB₂ at this temperature. This is supported by the thickness of the oxidized layer for ceramics containing 30 vol% TaSi₂ after oxidation at 1400° and 1500°C (50 and 60 μm compared with 300 and 600 μm for pure ZrB₂, respectively). A small increase in the thickness of the oxidized layer for the TaSi₂-containing material between 1400° and 1500°C together with 5–10 times higher thickness for pure ZrB₂ at these temperatures are additional and conclusive indications of the protective capabilities of Ta₂O₅-containing borosilicate glass. The SEM/EDS of the oxidized surfaces of all the ZrB₂-TaSi₂ samples showed glass immiscibility (similar to that for the ZrB₂-Ta₅Si₃ ceramics) with a Zr-containing glassy phase and the crystalline phase containing mostly Zr with a small amount of Ta. The XRD of the oxidized surface of the samples showed the presence of ZrO₂ and TaZr_{2.75}O₈. No Si- and B-containing crystalline phases were identified.

Figure 11 shows the behavior of the most oxidation-resistant compositions from each series of Si-containing additives characterized in this research together with oxidation data previously reported for ZrB₂/25 vol% SiC modified with 10 mol% TaB₂.¹⁶ An inset presents a magnified picture corresponding to the mass gains at 1200°–1400°C. All the compositions exhibited improved oxidation resistance at 1200° and 1300°C compared with the ZrB₂-SiC ceramics. The improved oxidation resistance persists with some of the compositions approaching 1400°C, with the best performance shown by the ZrB₂/SiC/TaB₂ material. As discussed above, the lower oxidation resistance of the SiC-containing ceramics below 1300°–1400°C compared with all other materials can be attributed to the insufficient oxidation of SiC at these temperatures to form a continuous protective borosilicate glass, while the significant oxidation of ZrSi₂, Ta₅Si₃, and TaSi₂ occurred at much lower temperatures. The presence of transition-metal oxides in the borosilicate glass, inducing immiscibility, additionally increased glass-protective capability. The diminishing effect of these oxides at temperatures above

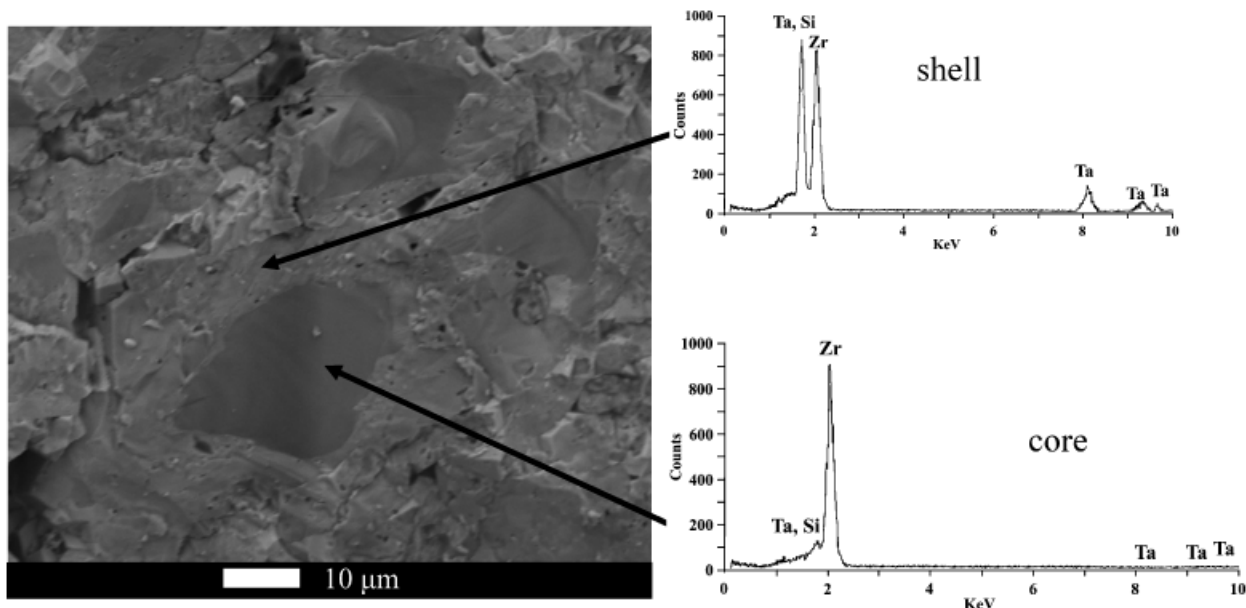


Fig. 9. SEM/EDS of ZrB₂/30 vol% TaSi₂ ceramics HP at 2000°C for 20 min, BS image.

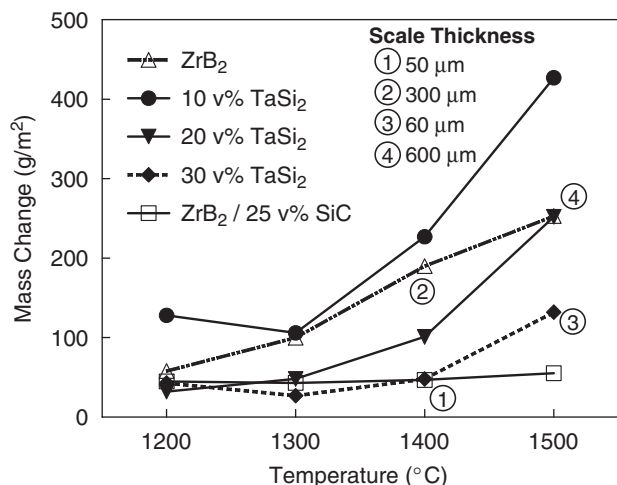


Fig. 10. Mass changes during furnace oxidation (2 h) of ZrB_2 ceramics containing 10, 20, and 30 vol% $TaSi_2$ at 1200–1500°C.

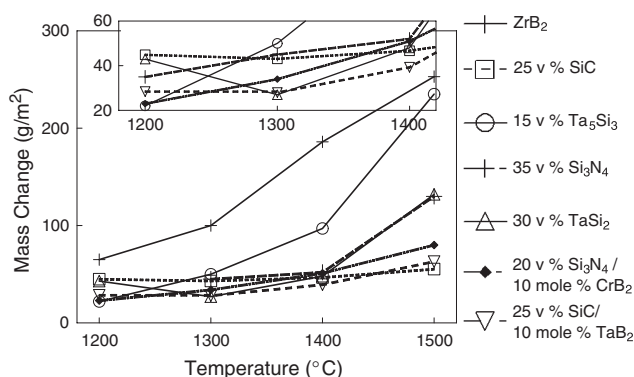


Fig. 11. Mass changes during furnace oxidation (2 h) of ZrB_2 ceramics containing SiC, Si_3N_4 , $TaSi_2$, and Ta_5Si_3 at 1200–1500°C.

1400°C and the increase in oxidation rates could be related to a decrease in glass viscosity, which leads to the reduction of immiscibility effects and an increase in oxygen diffusivity through the glass layer.

IV. Summary

Silicon carbide is conventionally used to improve the mechanical properties and oxidation resistance of ZrB_2 ceramics. The effect of SiC on the oxidation resistance of ZrB_2 is due to the formation of protective surface borosilicate glass, which enhances oxidation protection by acting as a barrier to the inward diffusion of oxygen. The effect of Si_3N_4 , Ta_5Si_3 , and $TaSi_2$ (as sources of Si instead of SiC) on the phase composition, microstructure, and oxidation behavior of ZrB_2 ceramics was characterized. Silicon nitride decomposed during the processing of ZrB_2 - Si_3N_4 compositions, and the final ceramics contained ZrB_2 , BN, $ZrSi_2$, and ZrN. Oxidation resistance of Si_3N_4 -modified ceramics increased with increasing Si_3N_4 content and was further improved by the addition of Cr and Ta diborides due to phase separation of the surface glass. The ZrB_2/Ta_5Si_3 materials exhibited complex chemical interactions and solid solubility between the components during hot pressing. Limited solid solubility was also observed between ZrB_2 and $TaSi_2$. Both Ta silicides significantly improved oxidation resistance of pure ZrB_2 ceramics, with the best performance exhibited by ZrB_2 containing 15 vol% Ta_5Si_3 and 30 vol% $TaSi_2$. The effect is attributed to the pronounced immiscibility in the surface glass formed during the oxidation tests. All studied compositions exhibited improved oxidation resistance below 1400°C compared with ZrB_2/SiC . At 1500°C, the SiC-modified ZrB_2 composition

performed best, but was only slightly better than the $ZrB_2/SiC/TaB_2$ and $ZrB_2/Si_3N_4/CrB_2$ ceramics.

Acknowledgments

The authors would like to acknowledge ONR (Drs. S. Fishman and D. Shifler) for providing support for this project and Dr. B. Varshal for valuable discussions on phase separation in glasses.

References

- M. M. Opeka, I. G. Talmy, and J. A. Zaykoski, "Oxidation-based Materials Selection for 2000°C+ Hypersonic Aerosurfaces: Theoretical Considerations and Historical Experience: Special Section: Ultra-High Temperature Ceramics (Guest Editors: Joan Fuller and Michael D. Sacks)," *J. Mater. Sci.*, **39** [19] 5887–904 (2004).
- W. G. Fahrenholtz, G. E. Hilmas, I. G. Talmy, and J. A. Zaykoski, "Refractory Diborides of Zirconium and Hafnium," *J. Am. Ceram. Soc.*, **90** [5] 1347–64 (2007).
- R. E. Loehman, "Ultrahigh-Temperature Ceramics For Hypersonic Vehicle Applications," *Ind. Heating*, **71** [1] 36–8 (2004).
- S. R. Levine, E. J. Opila, M. C. Halbig, J. D. Kiser, M. Singh, and J. A. Salem, "Evaluation of Ultra-High Temperature Ceramics for Aero-propulsion Use," *J. Eur. Ceram. Soc.*, **22** [14/15] 2757–67 (2002).
- J. R. Fenter, "Refractory Diborides as Engineering Materials," *SAMPE Quart.*, **2** [3] 1–15 (1971).
- E. V. Clougherty, D. Kalish, and E. T. Peters, "Research and Development Oxidation Resistant Diborides"; Technical Report AFML-TR-68-190, Manlabs Inc., Cambridge, MA 1968.
- A. L. Chamberlain, W. G. Fahrenholtz, G. E. Hilmas, and D. T. Ellerby, "Characterization of Zirconium Diboride for Thermal Protection Systems," *Key Eng. Mater.*, **264–268**, 493–6 (2004).
- I. G. Talmy and J. A. Zaykoski, "Properties of Ceramics in the $ZrB_2/ZrC/SiC$ System Prepared by Reactive Processing," *Ceram. Eng. Sci. Proc.*, **19** [3] 105–12 (1998).
- W. C. Tripp, H. H. Davis, and H. C. Graham, "Effect of SiC Additions on the Oxidation of ZrB_2 ," *Ceram. Bull.*, **52** [8] 612–6 (1973).
- J. W. Hinze, W. C. Tripp, and H. C. Graham, "High-Temperature Oxidation of a HfB_2 Composite," *J. Electrochem. Soc.*, **122** [9] 1249–54 (1975).
- E. V. Clougherty, R. L. Pober, and L. Kaufman, "Synthesis of Oxidation Resistant Metal Diboride Composites," *Trans. Metals Soc. AIME*, **242**, 1077–82 (1968).
- R. F. Voitovich, E. A. Pugach, and L. A. Menshikova, "High Temperature Oxidation of Zirconium Diboride," *Sov. Powd. Met.*, **7** [6] 44–8 (1967).
- F. Monteverde and A. Bellosi, "The Resistance to Oxidation of an HfB_2 -SiC Composite," *J. Eur. Ceram. Soc.*, **25** [7] 1025–31 (2005).
- F. Monteverde and A. Bellosi, "Production and Characterization of Ultra Refractory HfB_2 -SiC Composites," *Ceram. Eng. Sci. Proc.*, **25** [4] 13–8 (2004).
- W. G. Fahrenholtz, G. E. Hilmas, A. L. Chamberlain, and J. W. Zimmermann, "Processing and Characterization of ZrB_2 -Based Ultra-High Temperature Monolithic and Fibrous Monolithic Ceramics," *J. Mater. Sci.*, **39** [19] 5951–7 (2004).
- I. Talmy, J. Zaykoski, M. Opeka, and S. Dallek, "Oxidation Behavior of ZrB_2 Ceramics Modified with SiC and Group IV–VI Transition Metal Diborides"; pp. 144–158, *Proceedings of the International Symposium on High Temperature Corrosion and Materials Chemistry III*, 2001–12, Edited by M. McNallan, and E. Opila. The Electrochemical Society Inc., Pennington, NJ, 2001.
- L. Kaufman and E. Clougherty, "Investigation of Boride Compounds for Very High Temperature Applications"; Report RTD-TDR-63-4096, Part 1, AFML, WPAFB, OH, Dec. 1963.
- I. Talmy, J. Zaykoski, and M. Opeka Unpublished data
- W. Vogel, *Glass Chemistry*, 2nd edition, Springer-Verlag, New York, (1994).
- F. P. Glasser, I. Warshaw, and R. Roy, "Liquid Immiscibility in Silicate Systems," *Phys. Chem. Glasses*, **1**, 39–45 (1960).
- B. G. Varshal, "A Structural Model for Immiscibility in Silicate Glass-Forming Melts," *Glass Phys. Chem.*, **19** [2] 107–10 (1993).
- B. G. Varshal (ed.), *Two-Phase Glasses: Structure, Properties, and Applications*. AN SSSR, Nauka, Leningrad, 11–33, (1991).
- A. Bellosi and F. Monteverde, "Ultra-Refractory Ceramics: The Use of Sintering Aids to Obtain Microstructure Control and Properties Improvement," *Key Eng. Mater.*, **264–268** [Part 2] 787–92 (2004).
- K. Sato, H. Kakisawa, Y. Kagawa, H. Kaya, O. Funayama, and T. Isoda, "Reaction between Newly-Developed Si_3N_4 Fiber and Various Ceramics," *J. Mater. Sci. Lett.*, **19** [13] 1179–83 (2000).
- P. Shaffer, "An Oxidation Resistant Boride Composition," *Ceram. Bull.*, **41** [2] 96–9 (1962).
- P. Shaffer, "Oxidation-Resistant Ceramics and Method of Manufacturing Same"; U.S. Patent 3, 189, 477 (1965)
- V. A. Lavrenko, A. D. Panasyuk, T. G. Protsenko, V. P. Dyatel, E. S. Lugovskaya, and E. I. Egorova, "High-Temperature Reactions of Materials in the ZrB_2 - $ZrSi_2$ System with Oxygen," *Sov. Powder Metal Ceram.*, **21** [6] 471–3 (1982).
- A. D. Panasyuk, L. A. Glebov, T. G. Protsenko, K. M. Timofeeva, and V. P. Dyatel, "High-Temperature Oxidation of Materials in the System ZrB_2 - $CrSi_2$ "; pp. 127–30 in *Vysokotemp. Boridy Silitsidy*, Edited by T. Ya. Kosolapova. Naykova Dumka, Kiev, USSR, 1978.
- H. Pastor and R. Meyer, "An Investigation of the Effect of Additions of Metal Silicides on Titanium and Zirconium Borides from the Point of View of their

Sintering Behavior and their Resistance to Oxidation at High Temperatures," *Rev. Int. Hautes Temp. Refract.*, **11** [1] 41–54 (1974).

³⁰E. Opila, S. Levine, and J. Lorincz, "Oxidation of ZrB₂- and HfB₂-Based Ultra-High Temperature Ceramics: Effect of Ta Additions," *J. Mater. Sci.*, **39** [19] 5969–77 (2004).

³¹I. Talmy, J. Zaykoski, M. Opeka, and A. Smith, "Properties of Ceramics in the System ZrB₂-Ta₅Si₃," *J. Mater. Res.*, **21** [10] 2593–9 (2006).

³²T. J. Rocket and W. R. Foster, "Phase Relations in the System Boron Oxide–Silica," *J. Am. Ceram. Soc.*, **48** [2] 78 (1965).

³³S. S. Ordan'yan, A. I. Dmitriev, and E. S. Moroshkina, "Reaction of SiC with ZrB₂," *Inorg. Mater.*, **25** [10] 1487–9 (1989).

³⁴C. E. Brukl, "Ternary Phase Equilibrium in Transition Metal–Boron–Carbon–Silicon Systems. Part II. Ternary Systems, Volume X"; AFML-TR-65-2, Part II, Vol. X, Air Force Materials Laboratory, Wright Patterson Air Force Base, Dayton, OH, November 1966.

³⁵R. Kieffer and F. Benesovsky, "Recent Developments in the Field of Silicides and Borides of High-Melting-Point Transition Metals," *Powder Metal.*, [1/2] 145–71 (1958).

³⁶E. Parthe and J. T. Norton, "Phase Equilibria in M–X–X' and M–Al–X Ternary Systems (M = Transition Metal; X, X' = B, C, N, Si) and the Crystal Chemistry of Ternary Compounds," *Monatsh. Chem.*, **91**, 1127 (1960). □